General Disclaimer

One or more of the Following Statements may affect this Document

- This document has been reproduced from the best copy furnished by the organizational source. It is being released in the interest of making available as much information as possible.

- This document may contain data, which exceeds the sheet parameters. It was furnished in this condition by the organizational source and is the best copy available.

- This document may contain tone-on-tone or color graphs, charts and/or pictures, which have been reproduced in black and white.

- This document is paginated as submitted by the original source.

- Portions of this document are not fully legible due to the historical nature of some of the material. However, it is the best reproduction available from the original submission.

Analysis and Design of Optically Pumped Far Infrared Oscillators and Amplifiers

NASA Grant NGR 33-032-004

Period Covered: April 15, 1974 to April 15, 1978

Principal Investigator

T. A. Galantowicz
Dept. of Elec. Eng. and Computer Science
Union College
Schenectady, N.Y. 12308

NASA Technical Officer

Nelson McAvoy
NASA, Goddard Spaceflight Center
Greenbelt, Md.

Table of Contents

1. SUMMARY OF RESEARCH ACTIVITY

This report details the investigations and principal results of an experimental program to design and analyze the operation of optically pumped, waveguide, far infrared laser oscillators and amplifiers. These efforts were carried on at the Electrical Engineering and Computer Science Department of Union College, Schenectady, N.Y. supported by NASA Grant NGR 33-032-004.

a. Principal Results

i. A waveguide laser oscillator was designed and experimental measurements made of relationships among output power, pressure, pump power, pump frequency, cavity tuning, output beam pattern, and cavity mirror properties for various active gases.

ii. A waveguide regenerative amplifier was designed and gain measurements made for various active gases.

iii. An external Fabry-Perot interferometer was fabricated and used for accurate wavelength determination and for measurements of the refractive indices of solids transparent in the far infrared.

iv. An electronic system was designed and constructed to provide an appropriate error signal for use in feedback control of pump frequency.

v. Pump feedback from the FIR laser was decoupled using a vibrating mirror to phase modulate the pump signal. A marked improvement in FIR amplitude stability was noted.

b. Student Assistants

During the period of the grant the following electrical engineering

students assisted in the investigations:

David Proulx

Scott Landriau

Steven Rinehardt

Mark D. Rogers

Douglas S. Steele

Christos Skalkos

c. Publications and Papers

i. T. A. Galantowicz, - Waveguide Laser Amplifier Operation in the Submillimeter Wavelength Region," presented at Second International Conference and Winter School on Submillimeter Waves and their applications, Dec. 6-11, 1976, San Juan, Puerto Rico.

ii. T. A. Galantowicz, "An Optically Pumped Submillimeter Wavelength Regenerative Amplifier," IEEE Jour. of Quant. Elec., Vol. QE-13, p 459, June, 1977.

iii. Mark D. Rogers, "Regenerative Feedback Amplification in the Far Infrared," paper presented at 1977 Eastern Colleges Science Conference, Farleigh Dickinson University (awarded first prize in physics).

iv. T. A. Galantowicz, "Amplitude Stability Improvement of cw Submillimeter Wave Lasers with Phase Modulated Optical Pumping," (submitted to Optics Letters, June 1978).

2. FAR INFRARED OSCILLATOR STUDIES

a. Oscillator Fabrication

The far-infrared (FIR) laser oscillator cavity used in all experiments utilizes the waveguide configuration [1] shown in Fig. 1. The waveguide was fabricated from cylindrical lengths either of copper or of laboratory glass with inner diameters between 8 and 14 mm and lengths between 89 and 91 cm. The bores of the copper tubes were cleaned using an 8% solution of HCℓ to etch off the oxide coating. Both the glass and copper tubes were rinsed with methanol and dried with a wad of lint-free absorbent toweling. The pump input coupling mirrors were 2.5 cm diameter by 6.2 mm thick nickel coated mirrors with center holes with diameters of 1-2 mm. In some cases the mirrors were gold coated but this did not seem to cause any appreciable reduction in cavity losses. The FIR output mirrors were 2.5 cm diameter by 6.2 mm BK-7 glass flats gold coated on one side and with a 1.5 mm dia coupling hole in the center. The holes

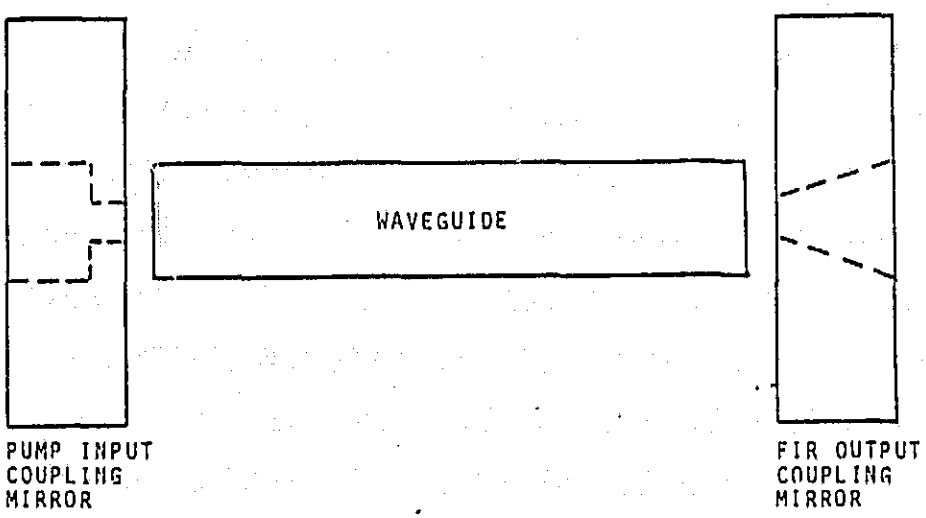

Fig. 1 FIR Oscillator Cavity Configuration

were tapered to a 30° included cone angle in order to improve coupling to output radiation modes. Metal mesh-dielectric mirrors [1-4] were employed as FIR output mirrors in the oscillator toward the end of the contract period and will be discussed later (see Sec. 2.c.)

The FIR cavity is housed in a 5.1 cm o.d. stainless steel vacuum jacket which is connected by brass bellows to Burleigh model SG101 mirror mounts at each end as seen in Fig. 2. The mirror mount holding the pump input coupling mirror has an assembly with a Brewster's window of ZnSe or KCℓ attached to it by an o-ring seal. This mount does not permit translation with respect to the optical cavity axis so the pump input mirror maintains a fixed separation of ≃ 1 mm from the end of the waveguide. The mirror mount holding the FIR output coupling mirror is mounted on an Oriel model B-62-60 translation stage to allow a variation of optical cavity length of up to 12 mm. The output coupling mirror assembly is

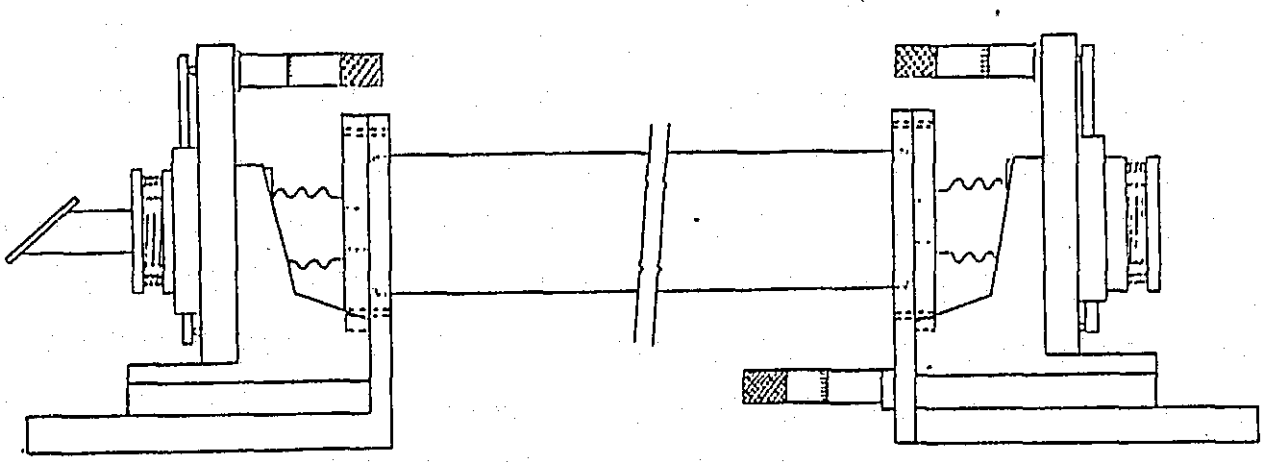

Fig. 2 FIR Oscillator

shown in detail in Fig. 3. The vacuum seal is completed with several o-rings and by a Z-cut quartz window which is transparent to the FIR radiation and opaque at the pump wavelengths.

Over the duration of the contract period this design has proven adequate as a source of submillimeter radiation with a variety of gases pumped cw with pump powers of the order of a few watts. The mechanical design could be improved significantly, however, by having the mirror mounts and translation stage internal to the vacuum jacket thus reducing the number of vacuum seals and the forces on the mirror mounts and translation stage. This is the design philosophy of the Advanced Kinetics Inc. laser vacuum boxes.

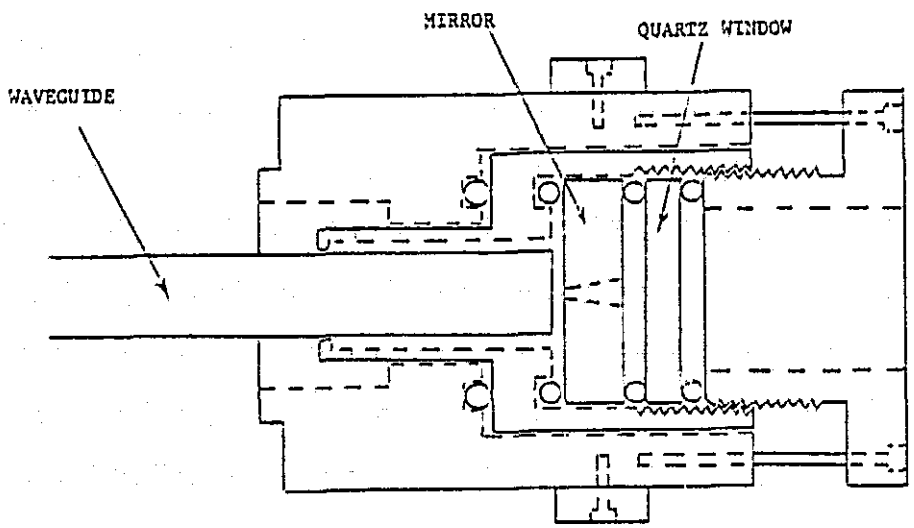

Fig. 3 FIR Oscillator output coupling assembly

b. Oscillator Experimental Arrangement

Operation of the oscillator required the experimental arrangement shown in Fig. 4. The pump source is a Molectron C-250 CO_2 laser with grating tuning and a piezoelectric translator to permit continuous tuning over a single line. Pump power is greater than 10 watts on more than 80 lines from 9.17 to 10.91 μm and greater than 20 watts on many lines near band centers. Several problems have been encountered in the course of operation of this laser: (a) initially it was found that the cooling water for the laser tube had to be distilled and deionized to get rid of a bothersome 60 Hz ripple in the output amplitude; (b) the ZnSe Brewster windows on the laser tube heat up and degrade mode quality;

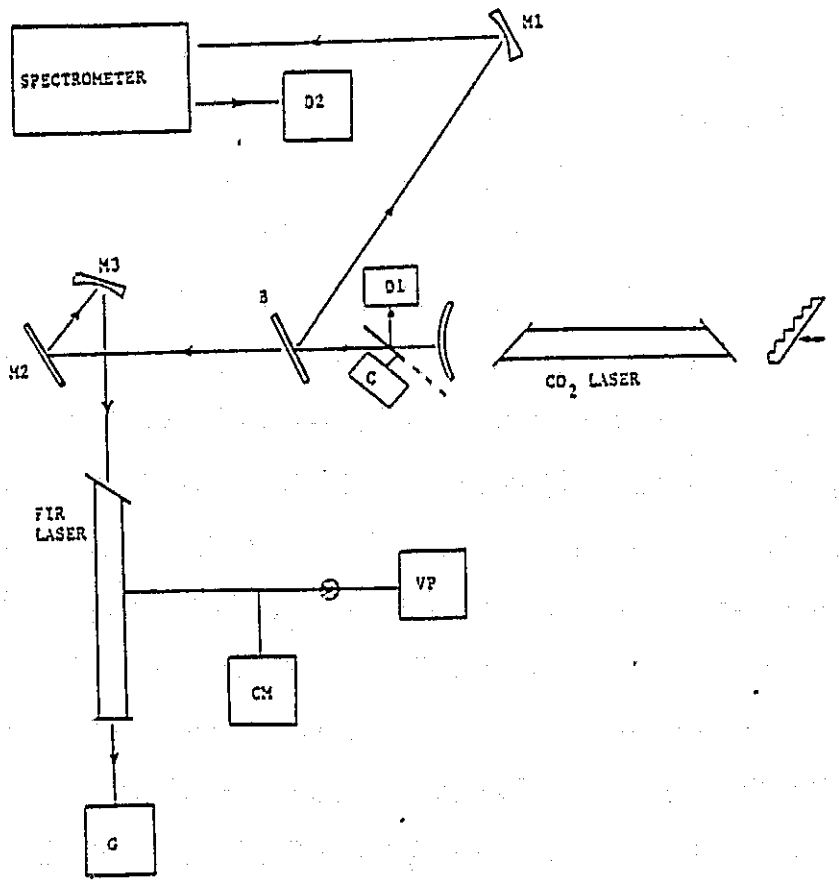

Fig. 4 FIR Oscillator experimental setup with mirrors M1, M2, M3; beamsplitter B; detectors D1, D2 and Golay cell G; chopper C; vacuum pump VP and capacitance manometer CM.

(c) attempts to frequency lock the output of the pump to the FIR output maximum (described in Sec. 5) have been unsuccessful due to the large hysteresis in the CO_2 cavity length tuning which is believed to be related to the thermal and mechanical design of the CO_2 laser. The laser output, however, does stay reliably on one line.

The pump radiation is externally chopped at 15 Hz by a chopper with a 50% duty cycle. A KCl beamsplitter (B in Fig. 4) reflects a portion of the pump beam off focusing mirror M1 and into a Jarrel Ash 1/2-meter spectrometer to monitor the pump wavelength. A Coherent Radiation Model 201 power meter is used to monitor pump power level. About 90% of the pump beam passes through beamsplitter B and is reflected off flat mirror M2 and a 1 meter radius mirror M3 which focuses the pump beam through the FIR input coupling hole. Mirror M3 is mounted in a 3 inch speaker cone and vibrates at low audio frequencies to decouple the pump feedback from the FIR laser cavity (See Sec. 7).

The FIR laser is evacuated using a mechanical roughing pump connected through appropriate valving and 3/8" copper tubing to the laser vacuum jacket. A base pressure of < 1 millitorr is possible as measured by an MKS Tru-Torr capacitance manometer. With the FIR cavity sealed off the leak rate is less than 0.5 mTorr per hour.

The FIR output is detected by an Oriel Golay cell with a 3 mm diamond window and 60° acceptance angle. The output can be observed directly on an oscilloscope or fed into a lock-in amplifier yielding a dc signal proportional to FIR output. The lock-in reference signal is derived from the output of a photocell mounted on the chopper. A pyroelectric detector has also been used as a fast detector of FIR output.

However, neither a lampblack coated SBN detector supplied by the Harshaw Chemical Co. nor a Molectron P3-01 detector responded to radiation at 372 μm while both operated satisfactorily at 119 μm.

Optical Alignment

Mirrors M2 and M3 in Fig. 4 were adjusted until the CO_2 pump beam was parallel with the axis of the FIR waveguide cavity. With a 1 meter radius mirror for M3 between 70-80% pump coupling efficiency was obtained with a TEM_{00} mode. Coupling efficiency was measured by comparing pump power reflected from M3 with pump power exiting the waveguide cavity with the FIR output coupling mirror removed. A He-Ne laser separated about 8 meters from the output end of the FIR laser was used to align the optical cavity. With the FIR output mirror removed, the beam incident on the pump input coupling mirror was reflected back on itself and parallel with the waveguide axis. The FIR output mirror was then replaced and the system pumped down. The glass output mirror was then aligned using the back side of the gold coating. This technique has always resulted in satisfactory alignment. In fact it was found that the cavity end mirrors could be rotated an angle of greater than 0.1° from the perpendicular to the cavity axis without appreciably affecting oscillator performance at FIR wavelengths as short as 119 μm. Small adjustments, however, have a noticeable effect on the beam pattern of hole coupled oscillators

c. Oscillator Parameter Measurements

A parameter study was undertaken to characterize the operation of the FIR oscillator. Table I lists the various output lines which were studied. No exhaustive attempt was made to determine all possible FIR output lines for each molecule nor was any attempt made to find new lines. Listings

of lines discovered for optically pumped FIR lasers are available in the literature [6-8].

The relationship between FIR output power, operating pressure, and pump power was studied. The results obtained for the 118.8 μm line of CH_3OH shown in Fig. 5 are characteristic of FIR optically pumped waveguide lasers. It can be seen from Fig. 5a that the maximum available pump power of 22 watts was insufficient to saturate the pump transistion even at pressures as low as 100 milli Torr. Since the pump absorption coefficients of most cw laser lines are in the range of 10^{-4} to 10^{-3} cm^{-1} at optimum pressure it is important to efficiently couple the pump energy to the active gas absorption transition [9]. Hodges et al have studied methods to optimize coupling efficiency [10-13]. Precise measurements of absorption

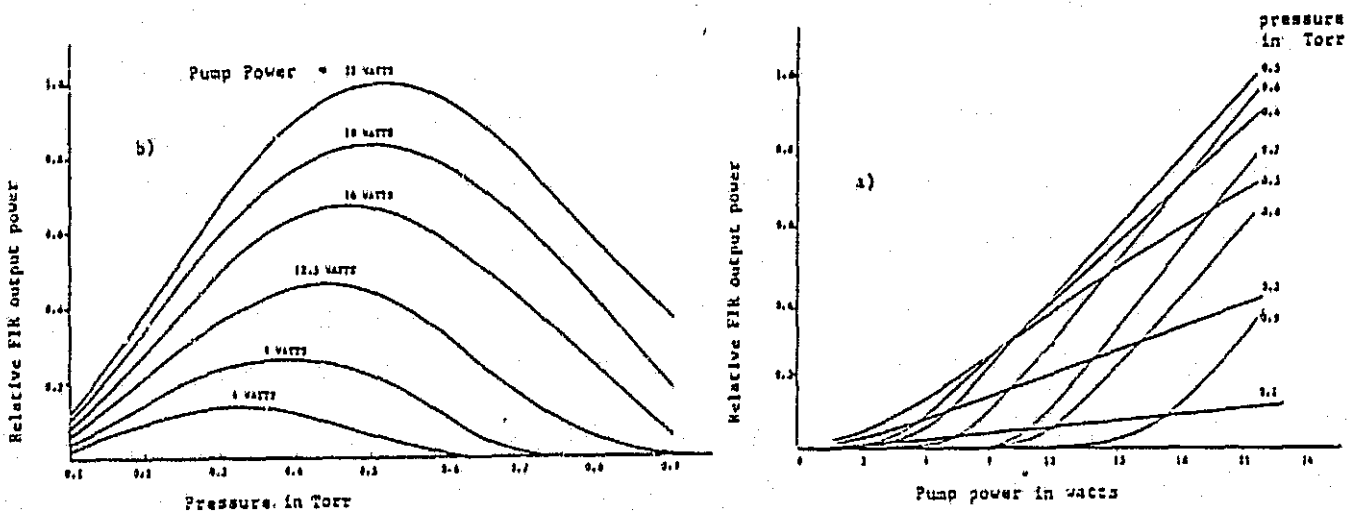

Fig. 5 FIR Output power versus (a) pump power and (b) pressure for the 118.8 μm line of CH_3OH

GAS	CO_2 Line	Pump 2 (μm)	FIR 2 (μm)	Pressure (mTorr)
CH_3F	P(20)	9.552	496	100
$C_2H_2F_2$	P(12)	10.512	375	300
	P(14)	10.532	415	250
	P(14)	10.532	554.4	120
	P(22)	10.6114	890	100
$C_2H_4F_2$	P(20)	10.591	458	150
CH_3CN	P(20)	10.591	372.9	150
CH_3OH	P(36)	9.695	118.8	400
	P(36)	9.695	170.6	
	P(16)	9.520	570.5	200

Table I

FIR Maser Output Lines

coefficients and pump saturation intensities have been determined by Weiss [14] for selected FIR laser gases. For the 119 μm transition in CH_3OH the pump transition has an absorption coefficient of .011 cm^{-1} $Torr^{-1}$ and a saturation intensity of 169 Watt / ($cm^2 Torr^2$).

The variation in output power with pressure given by Fig. 5b shows that there is a pressure optimum which is dependent on pump power and waveguide diameter. The output power drops when the optimum pressure is exceeded because the rate of relaxation from the excited vibrational state is not sufficiently fast to prevent thermalization of the rotational state populations by collisions. [10,15]. The waveguide diameter dependence is observed experimentally and is thought to be due to the fact that the vibrational relaxation rate is dominated by diffusion to the walls and is thus proportional to $(\text{diameter})^{-2}$. [15].

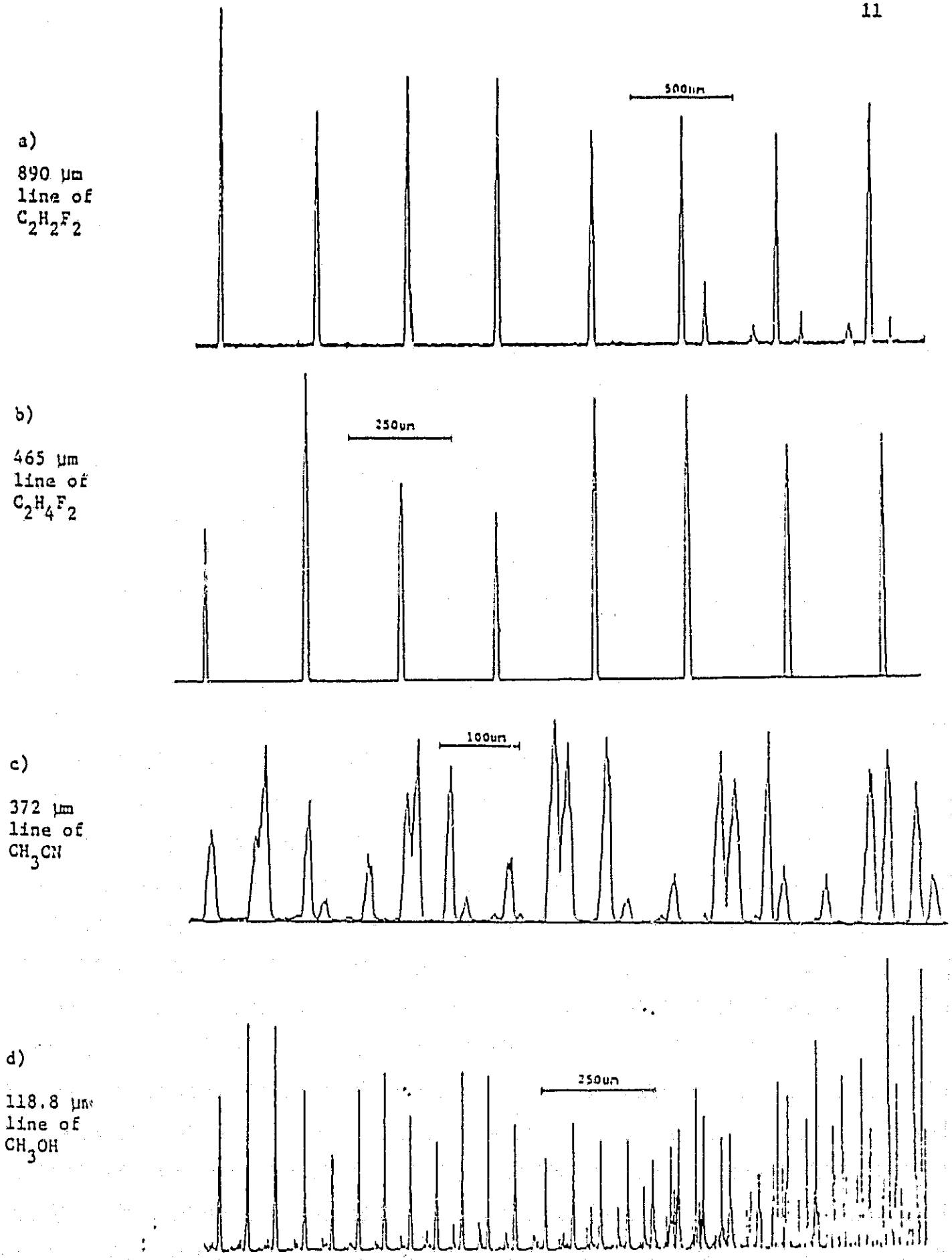

Fig. 6 FIR power output versus cavity length for various gases.

The variation of FIR output power versus cavity length was studied for several gases. The cavity length was changed by attaching a 2 r.p.m. motor to the micrometer of the translation stage which held the FIR output coupling mirror. A d.c. voltage proportional to end mirror displacement was produced by a Trans-tek Inc. DC-LVDT. The cavity length scans shown in Fig. 6 are useful in determining the approximate FIR wavelengths and the number of modes which can oscillate. The metal waveguides generally exhibit a much more complex variation with cavity length than the glass waveguides because the glass guides exhibit much greater attenuation for higher order waveguide modes. In particular, the 118.8 μm line of CH_3OH produces a wealth of output lines when using an 8 mm i.d. copper waveguide as shown in Fig. 7a. The lines correspond to several higher order transverse modes and cascade transitions as well as output at 118.8 μm (lines labeled A) and at 170.6 μm (lines labeled B). In Fig. 7b a glass waveguide of the same diameter is used resulting in fewer output lines. The relative amplitude of the lines can be varied by adjusting the cavity mirror alignment or fine tuning the pump frequency.

The FIR output radiation pattern was plotted for several different output lines. The radiation pattern for two different cavity length settings is shown in Fig. 8 for the 372 μm line of CH_3CN. Hole coupling tends to discriminate against operation in the lowest order mode and the complex radiation patterns of Fig. 8 reflect that fact. It was found that a metal mesh-dielectric output coupling mirror results in a more nearly gaussian output radiation pattern with a much smaller angle of diffraction. The dielectric coating was done commercially (described in Sec. 4a) and acted as a reflector for the pump radiation

a) Copper Waveguide

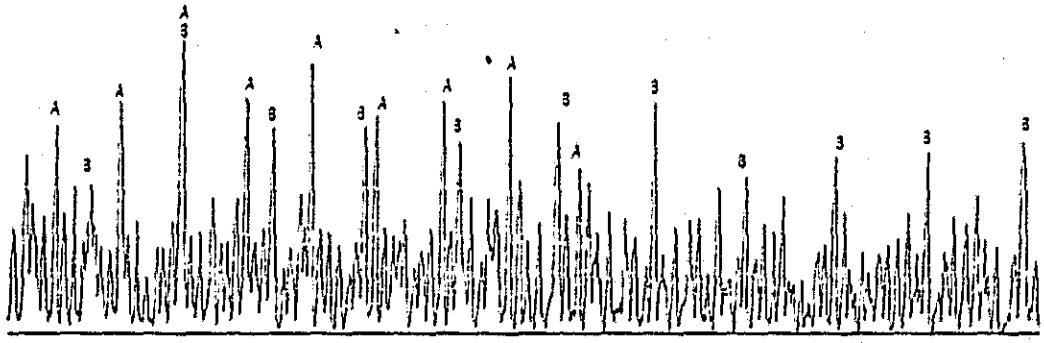

b) Glass Waveguide

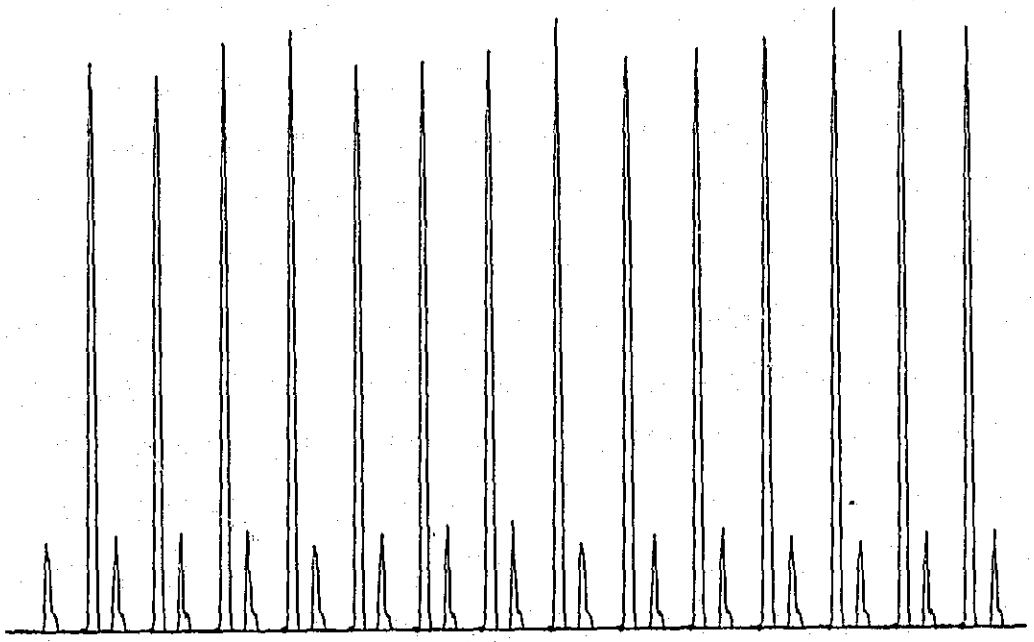

Fig. 7 FIR Output power versus cavity length for 8 mm waveguides. The active gas is CH_3OH pumped by the P(36) line of CO_2 at 9.895 μm.

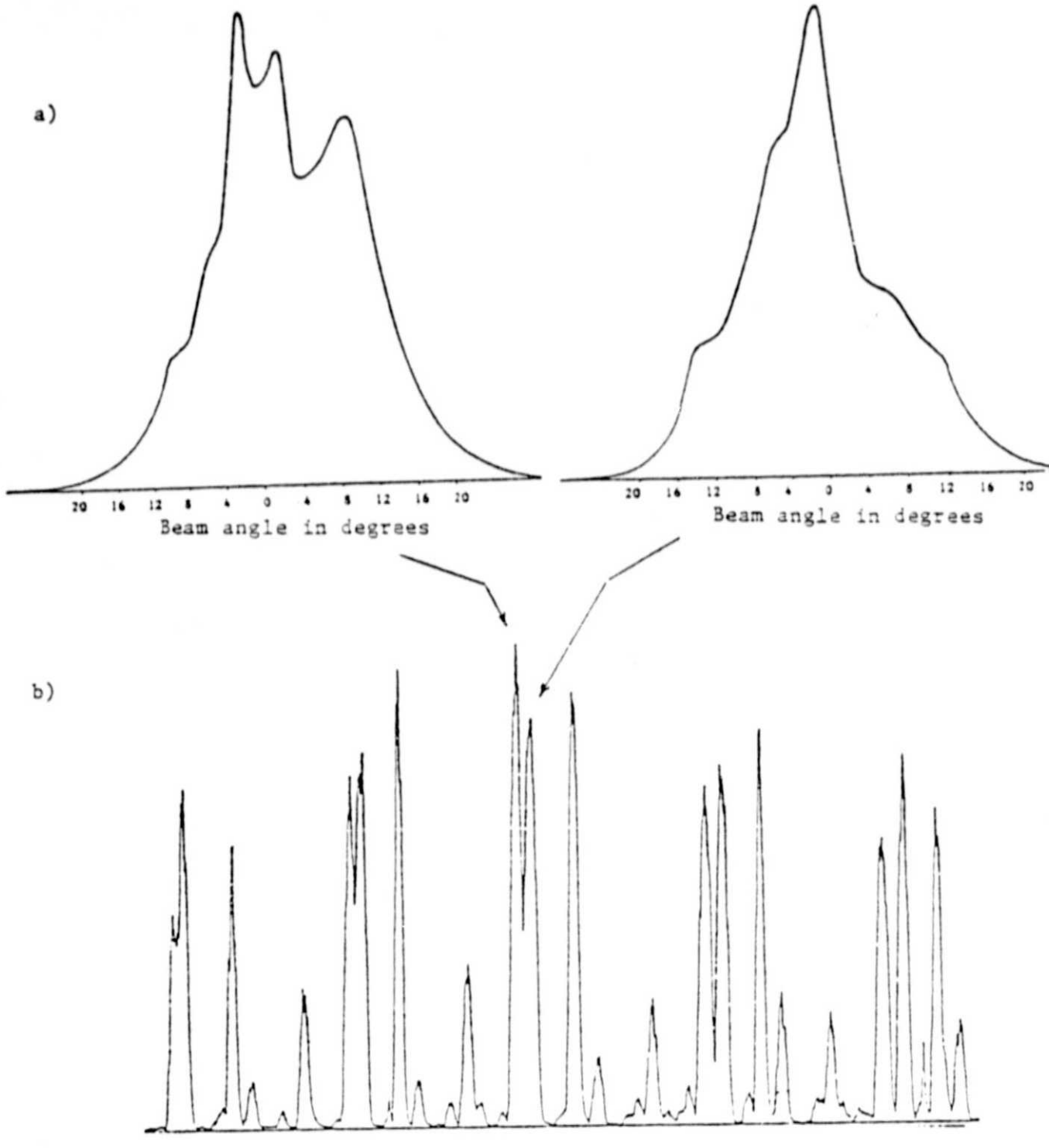

Fig. 8 (a) FIR output power versus angle from waveguide axis for output lines shown in (b). Fig. 8b is a plot of FIR output power versus cavity length for the 372 μm line of CH_3CN.

while transmitting 40-60% of the FIR radiation. A high vacuum system was employed to deposit a capacitive mesh gold coating on the dielectric to increase the FIR reflectivity. A metal mesh grid was used as a mask for the vacuum deposition.

3. FABRY-PEROT INTERFEROMETER

a. Wavelength Determination

An external Fabry-Perot interferometer (FPI) was constructed (a) to obtain accurate wavelength measurements of the FIR output radiation, (b) for possible use as a filter, and (c) for possible application in the determination of refractive indices of solids transparent at submillimeter wavelengths. The FPI was supported on a 50 cm granite bar and consisted of two metal mesh mirrors. One mirror was placed in a fixed mirror mount while the other was positioned on a motor driven linear translation stage. It was found that metal mesh of up to 1000 lines per inch could conveniently and reliably be stretched taut using the wire mesh holder sketched in Fig. 9.

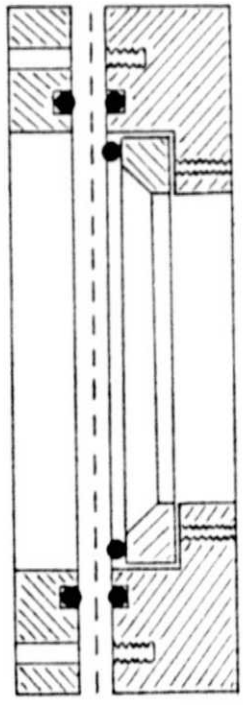

Fig. 9 Cross Sectional view of wire mesh holder. Three o-rings are used to hold the mesh taut.

The FPI has an aperture of 5.7 cm and was initially tested with one 333 line per inch and one 500 line per inch mesh. Using the 570.5 μm line from CH_3OH the FPI scan of Fig. 10a was obtained. At this wavelength the finesse of the interferometer is about 35 as compared with a calculated value of 40.7. To obtain a high enough finesse to resolve the 118.8 μm line in CH_3OH it was necessary to use two 1000 line per inch meshes resulting in the scan of Fig. 10b. The radiation wavelength is computed by using a dial indicator gauge with an accuracy of ±2.54 μm to measure the distance ℓ between the peaks at each end of the trace. If there are ρ peaks then the wavelength λ is given by

$$\lambda = 2\ell / (\rho-1) \qquad (1)$$

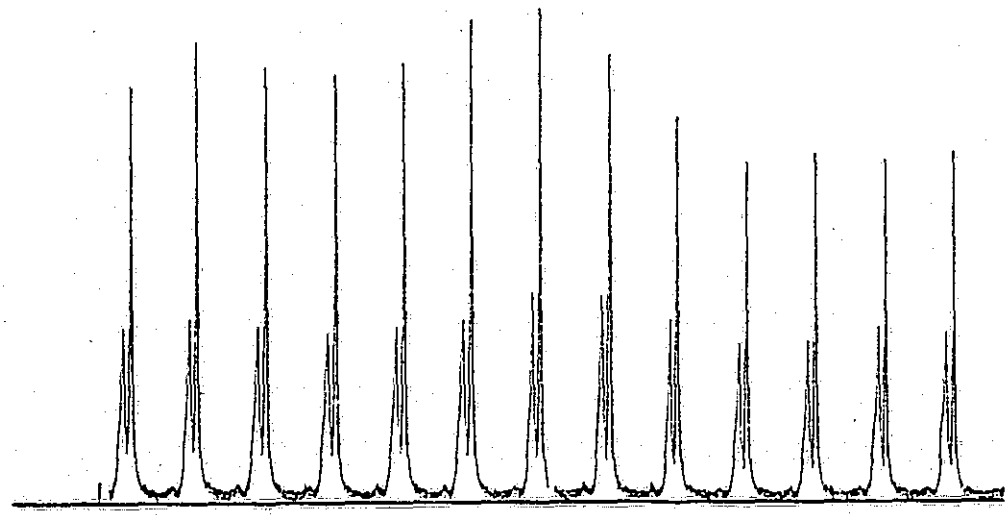

Fig. 10a FPI scan of 570.5 μm line of CH_3OH using one 333 line/inch and one 500 line/inch wire mesh.

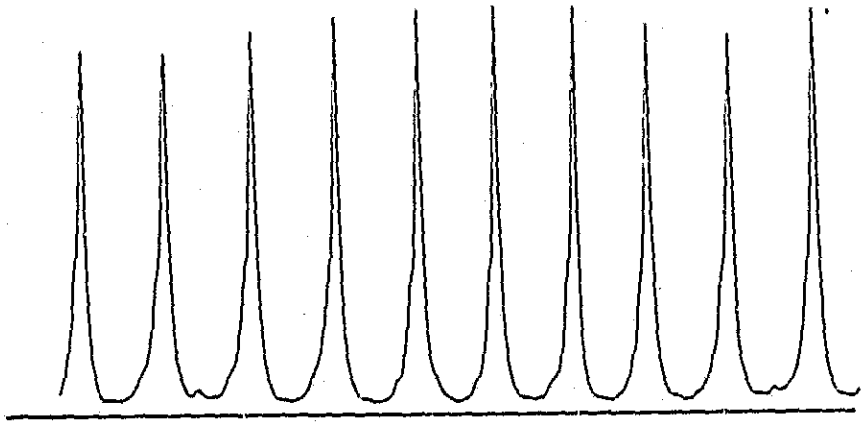

Fig. 10b FPI scan of 118.8 μm line of CH_3OH using two 1000 line/inch meshes.

The range of travel of the dial indicator was 10^4 μm. Thus for wavelengths less than 500 μm a wavelength measurement with an accuracy of better than ±0.1 μm was possible.

b. Refractive Index Measurements

Measurements of refractive indices of transparent solids of FIR wavelengths were made using an adaptation of the methods described by Chamberlain and Gebbie [16] and Lunazzi and Garavaglia [17]. It employes a Fabry-Perot interferometer in the arrangement shown in Fig.11. The FIR radiation which was collimated using a polyethylene lens, was incident on the FPI. A sample of index n and thickness t was mounted in a rotation stage between the FPI mirrors. The sample is initially made parallel with the FPI mirrors and the mirror spacing adjusted for maximum transmission. By rotating the sample through an angle θ the mirror spacing for maximum output shifts by an amount $\Delta\ell$ given by

$$\Delta\ell = t[1 - n - \cos\theta + (n^2 - \sin^2\theta)^{1/2}]. \qquad (2)$$

The most convenient method for making the measurement, however, is to keep the mirror separation fixed and find the angles θ_m at which the FPI transmission is a maximum. For these angles $\Delta\ell = m\lambda/2$ where m is an integer and the refractive index is given by

$$n = \frac{1}{2}[\sin^2\theta_m + (1 - \cos\theta - \frac{m\lambda}{2t})^2]/(1-\cos\theta - \frac{m\lambda}{2t}) \qquad (3)$$

In practice several values of θ_m can be measured for each sample and least squares curve fitting used to obtain a "best" value for n. The number of maximum transmission angles is limited by the size of the sample and decreases as the index of the sample gets larger [18].

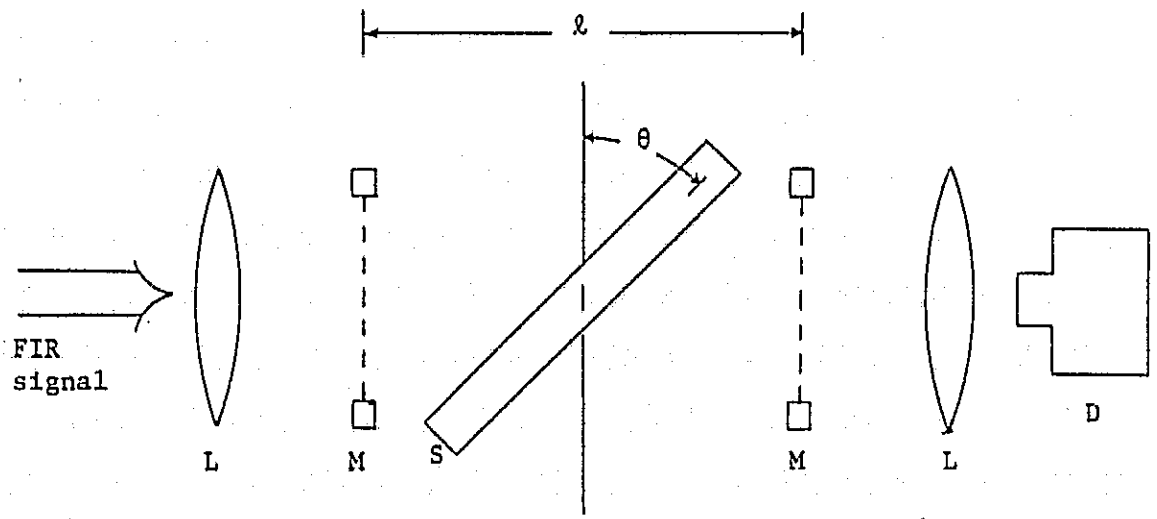

Fig. 11 Fabry-Perot metal mesh interferometer. Sample S is placed between mesh mirrors M. Radiation is collimated with lenses L and focused onto detector D.

Samples of polypropylene, polyethylene, and TPX were measured with results shown in Table II.

Material	Thickness (mm)	m_{max}	$n \pm \Delta n$
polypropylene	9.56	11	1.498 ± .005
polyethylene	9.68	12	1.49 ± .02
TPX	7.72	9	1.449 ± .01

Table II

Refractive Indices at λ = 496 μm

The index values computed separately for each angle θ_m in a given material showed a systematic error which was thought to be from thickness variations of the samples. The polyethylene sample in particular gave a large difference in calculated index from the smallest to the largest θ_m value. The precision of the refractive index values can be estimated from the sensitivity factors.

$$S_{\Delta\ell} = \frac{\partial n}{\partial(\Delta\ell)} = \frac{1}{2t}\left[\sin^2\theta/\left(1 - \cos\theta - \frac{\Delta\ell}{t}\right)^2 - 1\right] \tag{4}$$

$$S_t = \frac{\partial n}{\partial t} = -\left(\frac{\Delta\ell}{t}\right) S_{\Delta\ell} \tag{5}$$

$$S_\theta = \frac{\partial n}{\partial\theta} = \frac{1}{2}\sin\theta\left\{1 + \frac{2\cos\theta}{1-\cos\theta - \frac{\Delta\ell}{t}} - \frac{\sin^2\theta}{\left(1-\cos\theta - \frac{\Delta\ell}{t}\right)^2}\right\} \tag{6}$$

From these expressions it can be determined that the index value is most sensitive to errors in angle and errors in the initial positioning of the mirror separation at small angles (for low values of the integer m).

4. FIR REGENERATIVE AMPLIFIER

a. Amplifier Design

A regenerative FIR amplifier was designed and used to measure small signal gain. The amplifier waveguide cavity was composed of an 89.1 cm long by 13.3 mm diameter copper tube. A nickel plated metal end mirror with a center hole 1.7 to 2.0 mm in diameter was used as the pump input coupling mirror. The other end mirror was actually a pair of dielectric coated mirrors which acted as a Fabry-Perot interferometer. The amplifier cavity is shown in Fig. 12. The dielectric mirrors were commercially fabricated by Valtec Corp. and were composed of a multilayer coating of germanium and zinc-selenide on a 2.54 cm diameter by 3.2 mm thick E-cut quartz flat. The multilayer coating was specified to have a reflectivity greater than 98% at wavelengths between 9.5 and 10.6 μm.

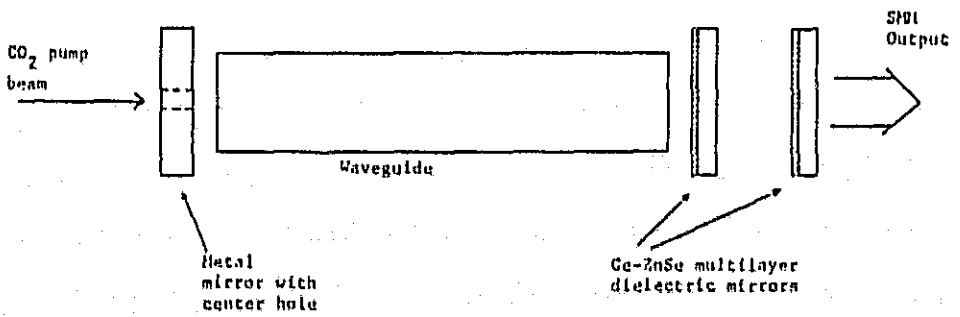

Fig. 12 FIR amplifier cavity configuration

It was decided to use the dielectric mirror interferometer for both input and output coupling of the FIR signal in order to: 1) maximize input and output apertures; 2) control reflectivity at the signal wavelength

so as to readily convert from an amplifier to an oscillator; 3) optimize signal coupling into the amplifier, and 4) maximize reflectivity at the pump wavelength. When only one of these mirrors was used as a FIR output mirror oscillation occurred readily at high gain transitions in CH_3OH, CH_3CN, and CH_3F. Transmission measurements indicated each mirror had 40-60% reflectivity at wavelengths between 100 and 500 μm. For amplifier operation it was necessary to adjust the interferometer mirror spacing to reduce the feedback gain. The transmission versus mirror spacing for the dielectric mirror pair was found to produce a variation of 6:1 at a wavelength of 373 μm as shown in Fig. 13.

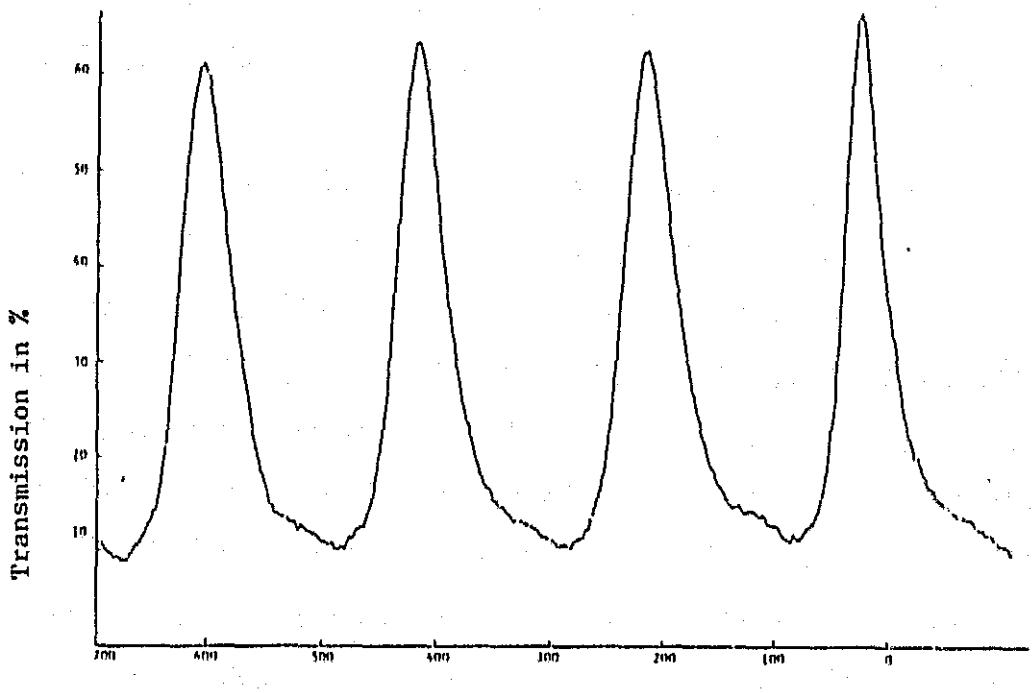

Fig. 13 Transmission versus dielectric mirror spacing at λ = 373 μm

The interferometer assembly was installed in the output mount using one mirror as a vacuum window as shown in Fig. 14. Mirror spacing was adjustable by rotating the threaded sleeve while mirror parallelism was

possible by varying the pressure of the mirror against the O-ring seal. The output mirror assembly was mounted in an Oriel Model 1750 adjustable angle mount as was the pump input coupling assembly. The Oriel mounts were then mounted through bellows seals to a stainless steel vacuum jacket similar to the assembly shown for the oscillator in Fig. 2.

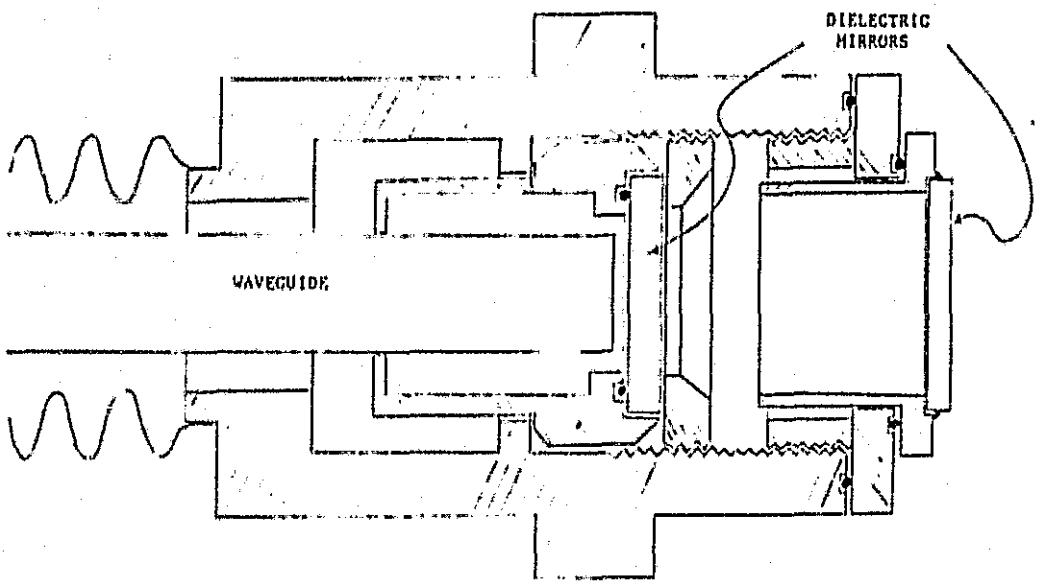

Fig. 14 FIR amplifier output assembly

The performance of this amplifier was found to be quite unstable. It was later found that the elastomer springs used in the Oriel mirror mount allowed the mirrors to vibrate in response to mechanical vibrations affecting the stability of CO_2 laser pump through pump feedback from the output coupling mirror.

b. Amplifier Experiment

Amplifier operation was studied using the experimental configuration shown in Fig. 15. The output from the CO_2 laser pump was split into two beams to provide the pump power for both the oscillator and the amplifier. Although not indicated in Fig. 15, both beams are focused to get greater

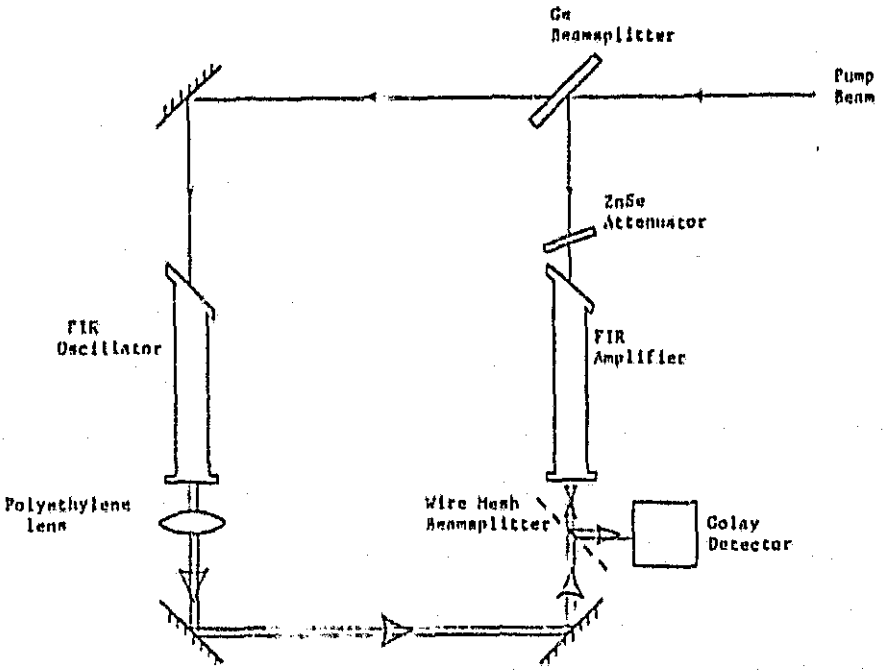

Fig. 15 FIR Amplifier experimental configuration

than 75% of the incident pump power through the holes in the pump input mirrors of the oscillator and amplifier. The amplifier pump beam can be attenuated by using the angle dependence of transmission through a ZnSe attenuator plate.

The FIR oscillator employed hole coupling through a 1.5 mm diameter hole. The oscillator output is collimated using a polyethylene lens

and the beam is aligned to pass down the bore of the amplifier waveguide using two mirrors. A portion of the signal is reflected by the amplifier dielectric-mirror interferometer while the remainder is coupled into the amplifier cavity. This signal is regeneratively amplified and coupled back out through the interferometer mirrors. The wire mesh beamsplitter directs both the amplified signal and the portion of the input signal reflected from the interferometer mirrors onto a Golay detector.

Amplifier operation was obtained by adjusting the amplifier for oscillation with the dielectric mirror interferometer adjusted for minimum reflectivity. Pump power was then reduced by rotating the ZnSe plate to a point just below oscillation threshold.

Amplifier gain was measured at three wavelengths: the 119 μm transition in CH_3OH, the 373 μm transition in CH_3CN and the 496 μm transition in CH_3F. Amplifier output versus time for the 373 μm transition is shown in Fig. 16.

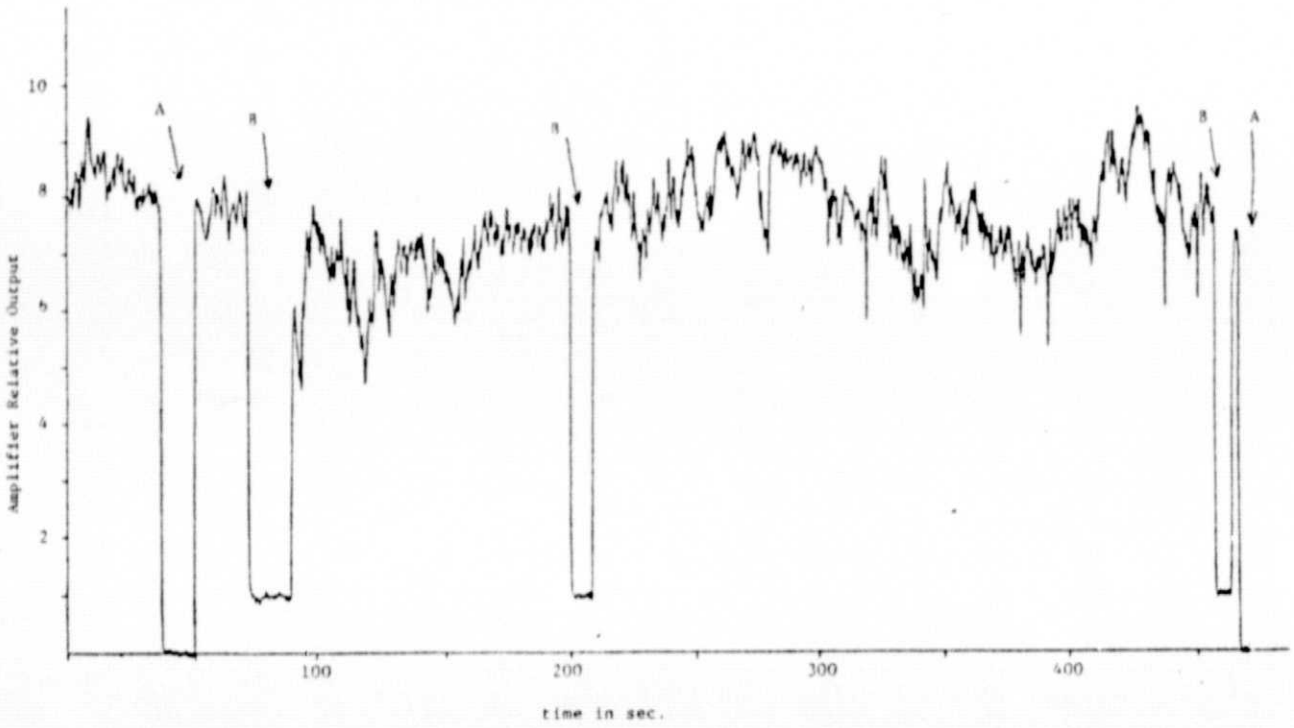

Fig. 16 Amplifier Output vs. time for the 373 μm transition in CH_3CN

The dips in output marked A correspond to times when the signal input to the amplifier was off and were used to check that the amplifier was not oscillating. Dips labelled B correspond to times when the pump power to the amplifier was turned off. Rapid variations in output power level are due to oscillator and amplifier cavity length variations. The gain is extremely sensitive to both oscillator and amplifier cavity length since these act as two coupled resonant cavities. Longer term output variations are due to pump frequency drift. The received signal with amplifier on was about nine times the signal without amplification. This is not the gain, however, since about one-third of the unamplified signal is reflected from the outside mirror of the dielectric mirror interferometer. The true gain is then about a factor of 12. A crude estimate of small signal gain α is given by [19]

$$G = (1-R)^2 \, e^{2\alpha\ell}/(1-Re^{2\alpha\ell})^2 \qquad (7)$$

Taking $R = .33$, $\ell = .891$ m, $G = 12$ we find $\alpha = .43\ m^{-1}$

The amplifier output versus time on the 119 μm CH_3OH line is shown in Fig. 17. For this case the gain is down to approximately 5 most likely

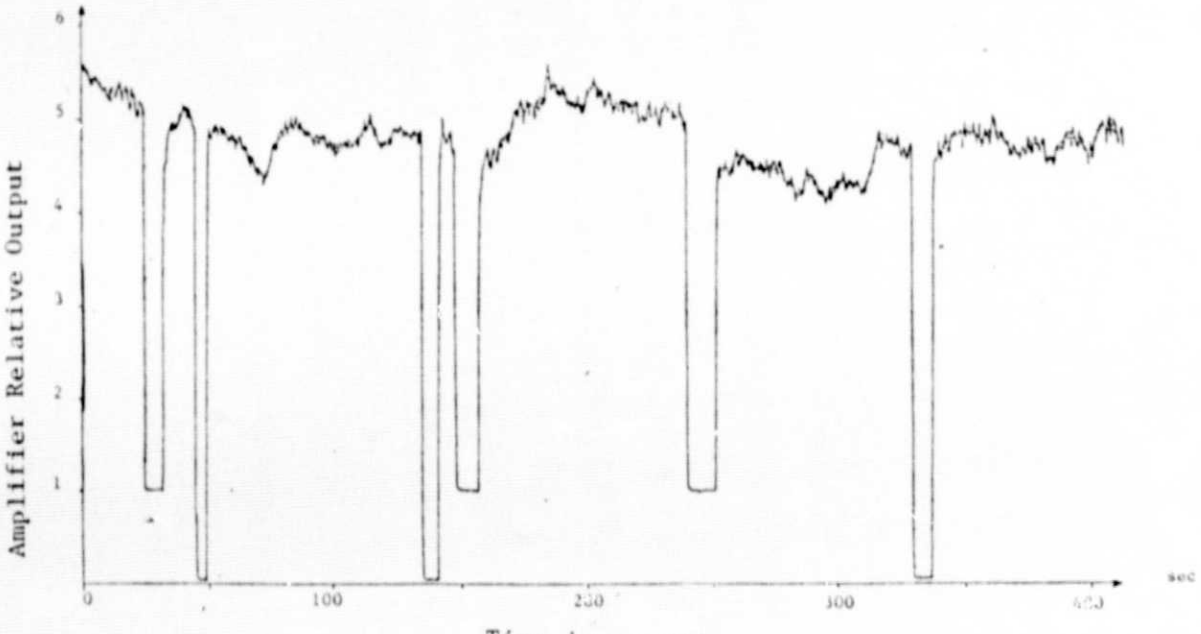

Fig. 17 FIR amplifier output versus time for the 119 μm line in CH_3OH

due to operating conditions which are less than optimum. Since oscillation occurs at very low pump powers (< 1 watt) even with low output mirror reflectivity it was necessary to operate at gas pressures which increased the oscillation threshold at the expense of small signal gain. For the case of the 496 μm transition in CH_3F this condition held in the extreme such that gains of only 2 to 4 were obtained for this transition.

5. PUMP FREQUENCY STABILIZATION

The FIR laser output amplitude stability is affected principally by pump laser frequency drift and by changes in FIR cavity length due to temperature. In a well designed oscillator cavity the thermal drift has a negligible effect on amplitude stability - at least in a laboratory environment. However, since a pump frequency drift on the order of ±10 MHz is sufficient to quench FIR laser action [6], it is important to stabilize the pump laser frequency. A variety of CO_2 laser stabilization methods are possible:

a) Commercial systems are available which make a polarity and amplitude comparison between an ac "dither" signal applied to the piezo electric cavity length tuning of the pump laser and the resulting ac component of laser output intensity produced as the cavity resonance scans the lineshape of the lasing transition. An error signal is developed to maintain the pump at line center.

b) The saturated CO_2 fluorescence technique developed by Freed and Javan [20] can be used to stabilize the pump frequency to the CO_2 line center.

c) A feedback signal can be derived from the dc discharge current of a CO_2 laser [21]

d) A dc signal derived from the FIR output amplitude may be used to control the pump cavity length tuning [22]

e) The opto acoustic effect [23-28] can be used to maintain the CO_2 pump at the center of the pump absorption line in the active FIR molecule.

Since the pump absorption line center is not generally the same as the CO_2 laser line center only methods d) and e) are generally useful for FIR laser applications.

An electronic system to stabilize the FIR amplitude by correcting for pump frequency drift as described by method d) above is shown in Fig. 18.

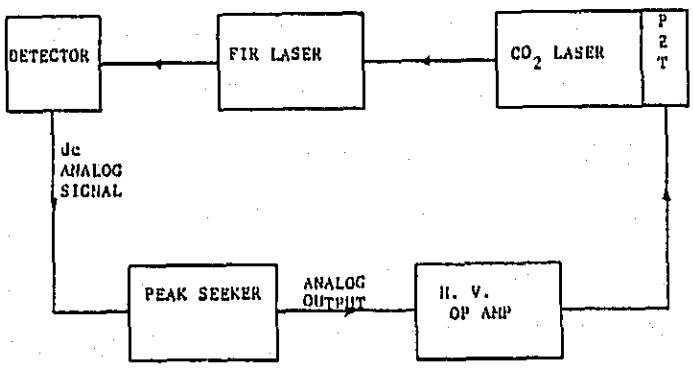

Fig. 18 FIR laser Stabilization System

The electronic component dubbed "peak-seeker-I" in Fig. 18 periodically samples the analog voltage (0 to 10 volts) which is proportional to FIR amplitude and produces an increasing or decreasing staircase output

which controls the cavity length of the CO_2 laser. Samples can be selected every T = 1, 2, 4 or 8 seconds. Consider two samples - s_t at time t and the next sample s_{t+T} at time t+T. If $s_{t+T} \geq s_t$ then the next step in the staircase output of the peak-seeker is 0.02 volts greater than the previous step. If $s_{t+T} < s_t$ then the next voltage step is 0.02 volts less than the previous step. The high voltage operational amplifier used to boost the voltage up to the levels needed to control the piezoelectric tuner is a Kepco OPS-500B power supply.

The schematic for the peak-seeker is given in Fig. 19. The input and reference voltage connections to the 8-bit A/D converter are not shown since they depend on the type and range of input signal.

Although the peak-seeker functioned perfectly, as did the open-loop portion of the system of Fig. 18 between the FIR laser and the PZT feedback input, the closed loop system failed to function properly. An experimental study of the relation of CO_2 laser output frequency to applied piezoelectric voltage revealed a large hysteresis as the PZT voltage was cycled over its range even for time intervals on the order of 1 second. Further attempts at this method of frequency stabilization were abandoned since it was felt that major modifications would be needed in the operation of the pump laser which would have prevented the completion of other experiments.

6. BUFFER GAS STUDIES

It has been found that the mixture of a buffer gas with the active molecule in a FIR laser can result in up to 50% increases in output power [29]. The buffer gas acts to improve the rate at which the population of the pumped vibrational state is decreased. The original buffer

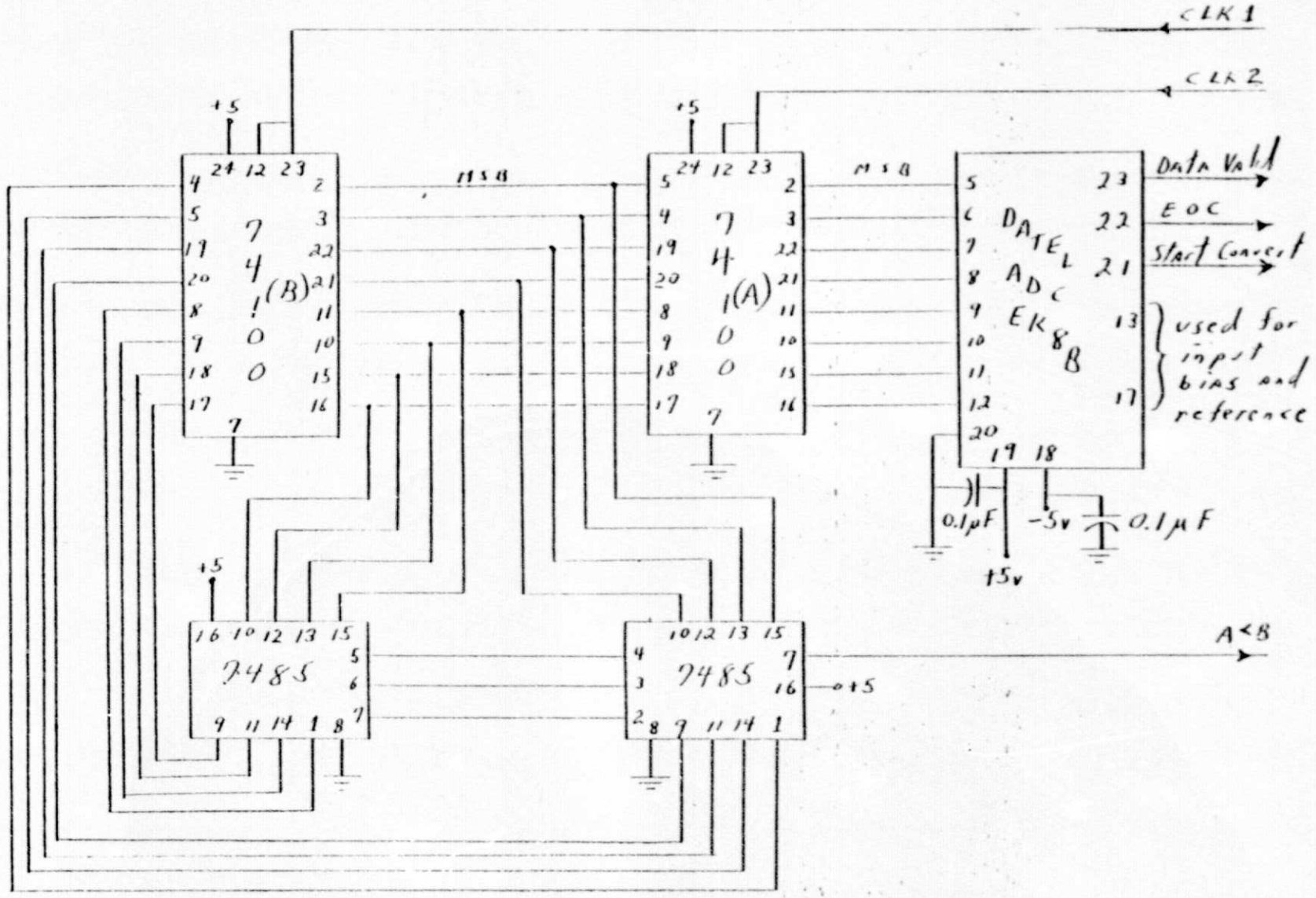

Fig. 19a Peak Seeker Sample and compare circuitry

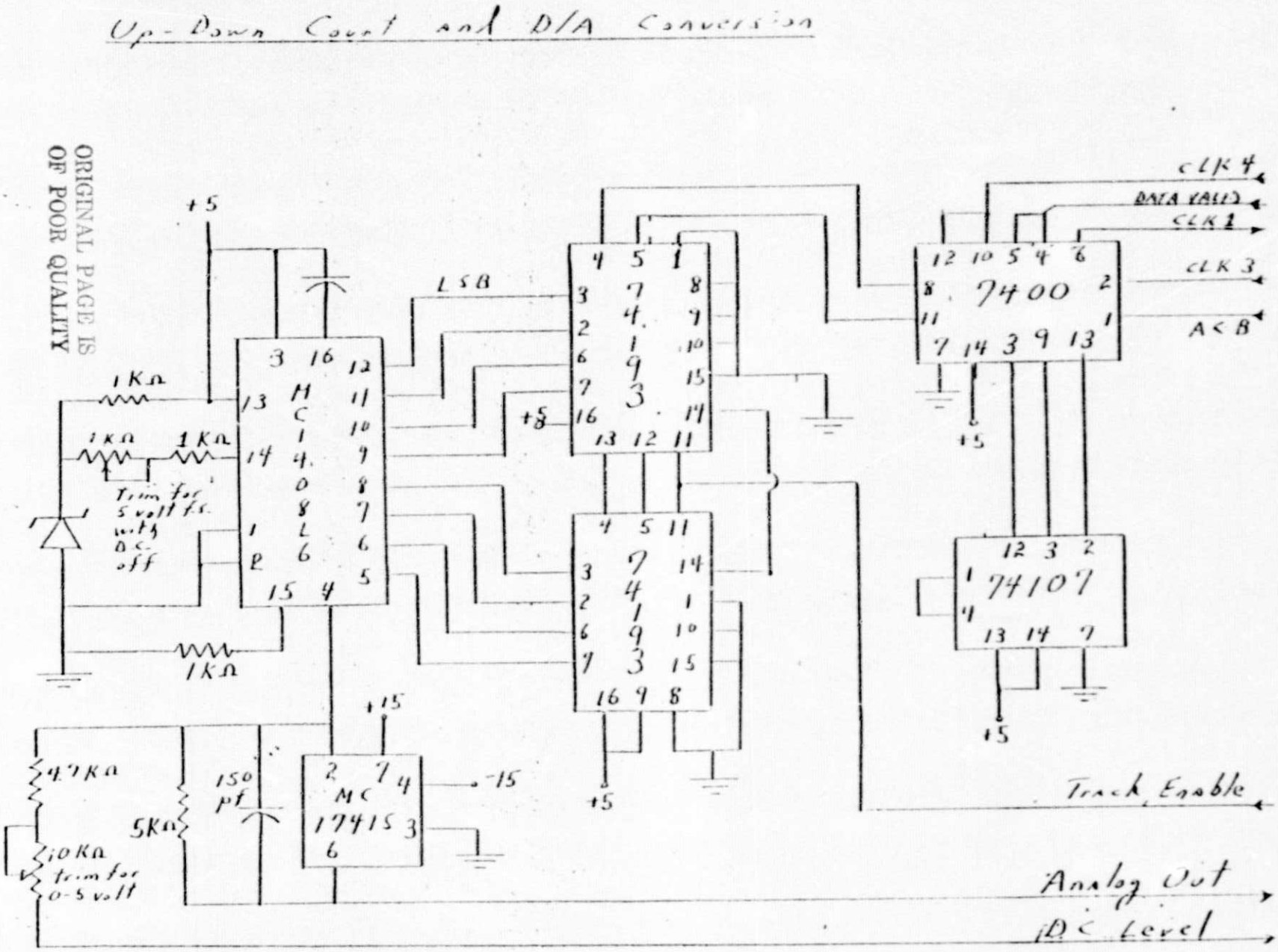

Fig. 19b Peak Seeker up/down counter and D/A conversion circuitry

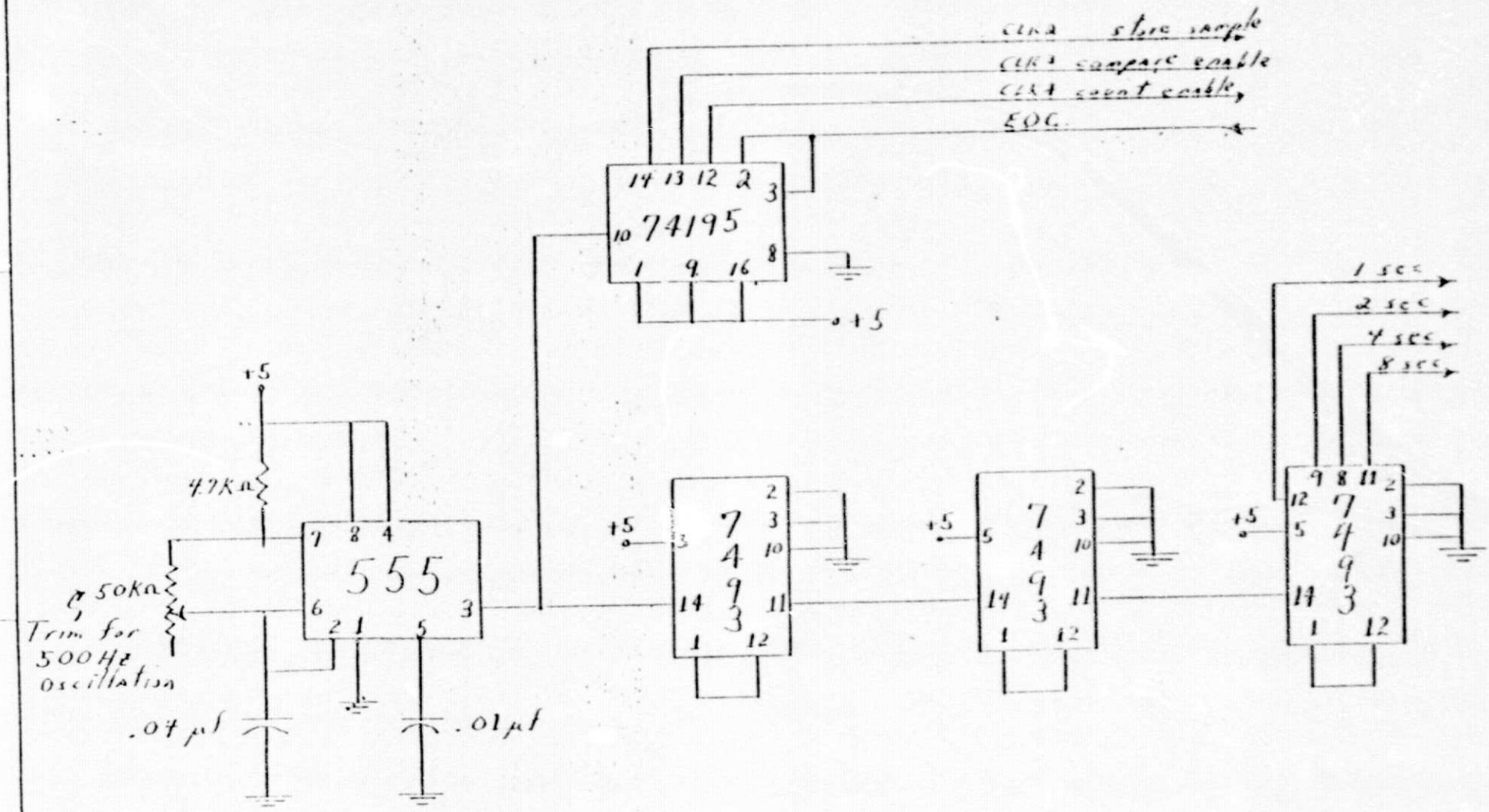

Fig. 19c Peak Seeker clock circuitry

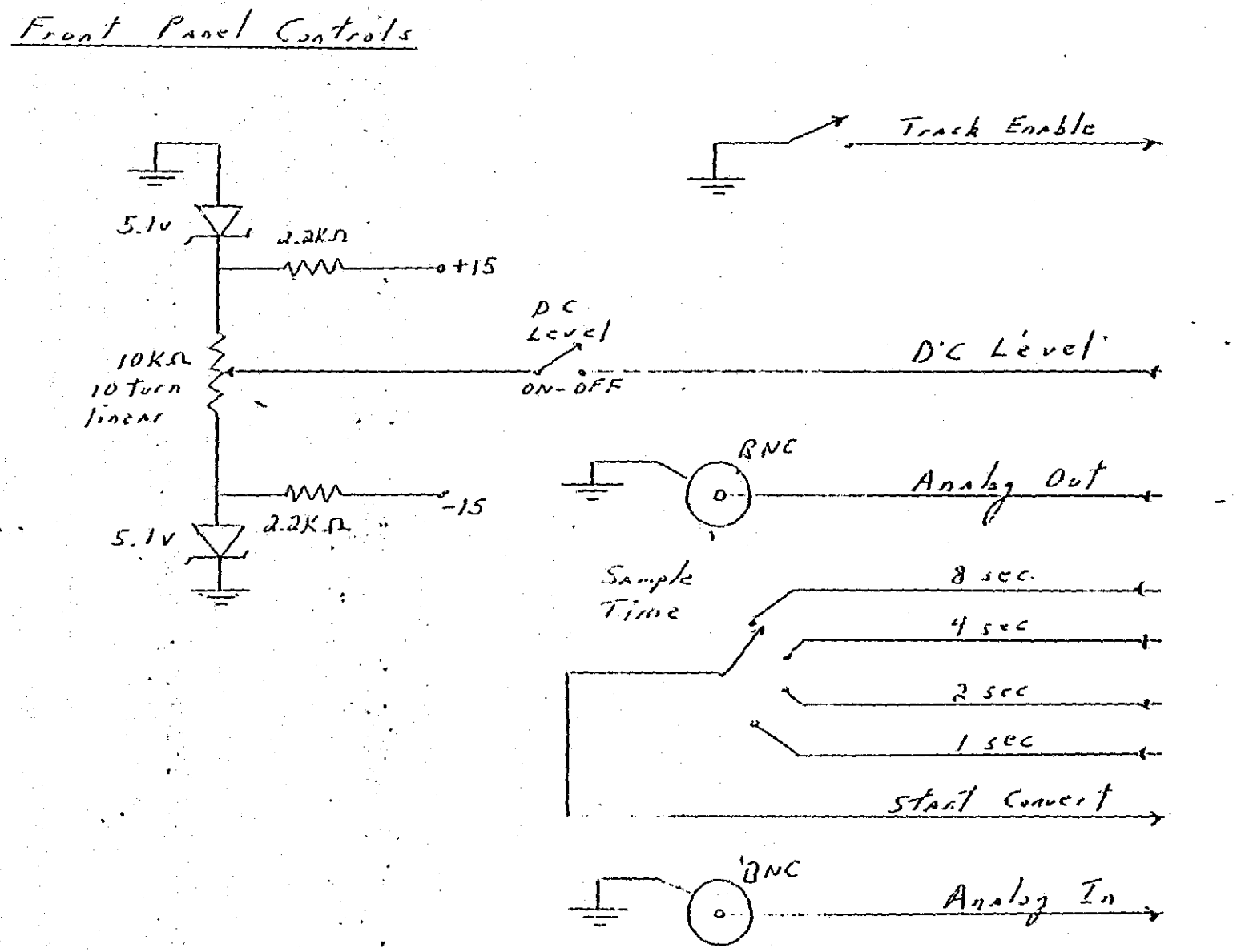

Fig. 19d Peak Seeker front panel controls

gas studies utilized a FIR laser with an open Fabry-Perot resonator and a flowing gas system. [29] Studies of the effects of buffer gases were undertaken using the waveguide laser of Fig. 1 and 2 in both the sealed off and flowing gas condition.

The vacuum system for the laser initially used only a single port to pump down the system and then bleed in the active gas. When this procedure was used to bleed in both the active gas and the buffer gas an improvement in output power was obtained only during the transient period when the buffer gas was added. This was due to inadequate mixing resulting from the use of a single vacuum port. The oscillator vacuum jacket and associated vacuum valving was modified to allow both flowing and sealed off operation. It was then possible to obtain the correct mixture of active and buffer gases.

Various mixtures of CH_3F with the buffer gas C_6H_{14} were studied with the following results:

a) The operation of the waveguide laser with buffer gas was qualitatively the same as for the open resonator of Ref. 29. An increase of about 50% in output power was obtained for approximately equal mixtures of active and buffer gas.

b) The output power improvement was the same for both flowing gas and sealed off systems. The improvement did not change with time in the sealed off system.

c) It appeared that the output amplitude was more stable with the presence of the buffer gas.

Since the results agreed in almost every aspect with the results of Chang and Lin [29] further buffer gas experiments were terminated.

7. PUMP FEEDBACK DECOUPLING

Optically pumped submillimeter wave lasers commonly utilize a geometry such as that shown in Fig. 4 in which the pump beam is aligned axially with the FIR cavity. In this arrangement the pump beam is coupled to the FIR laser cavity by focusing through a hole in the input mirror. The FIR output mirror is designed to have a high reflectivity at the pump wavelength and thus reflects a portion of the pump beam out the input coupling hole and back into the pump laser cavity. This feedback signal affects both the amplitude and frequency stability of the pump laser. Since pump frequency variations of the order ±10 MHz are sufficient to quench FIR laser action [6] the effects of pump feedback must be minimized in the design of an amplitude stable FIR laser.

One method to minimize instabilities caused by feedback - used by Hansch et al [30] in a dye laser system - employes a vibrating mirror to phase modulate the back-reflected signal. A 4:1 improvement in the amplitude stability of a FIR laser was realized using a vibrating mirror to decouple the pump beam reflected back to the CO_2 pump laser. An expression is derived for the peak frequency deviation of the pump laser due to a phase modulated feedback signal.

FIR laser amplitude stability was investigated using the arrangement of Fig. 4. A 2.5 cm gold-coated flat mirror (M2) was glued to the center of a commercially available 3-inch loudspeaker to phase modulate the back-reflected portion of the pump beam. The pump input was focused through a 2 mm hole in the pump input coupling mirror by a 50 cm focal length gold-coated mirror. The FIR laser cavity was formed by a 90 cm long, 14 mm diameter glass waveguide with a capacitive grid-dielectric output coupling mirror. With this arrangement it was estimated that

as much as 0.2% of the pump output could be reflected back into the CO_2 pump cavity.

Fig. 20 shows a comparison of FIR output power versus time with and without the vibrating mirror. The FIR signal is the 496 μm line of the CH_3F molecule pumped by the 9.55 μm P(20) line of the CO_2 laser. It is detected by a Golay cell which drives a lock-in amplifier. An approximately 4:1 reduction in rms output amplitude fluctuation is realized with the mirror vibrating at 100 Hz. This result was found to hold over the range of frequency response of the speaker for vibration amplitudes in excess of one-quarter of the pump wavelength. The change in average amplitude from the stationary (A) to the vibrating (B) mirror condition seen in Fig. 20 is due to a dc shift in pump frequency caused by asymmetric mirror vibration. It can be eliminated by readjusting the fine tuning of the pump laser cavity length. The spikes which occur in going from the vibrating to the stationary mirror conditions are due to switching transients picked up by the electronics.

Higher frequency fluctuations in FIR output power were investigated using a pyroelectric detector to measure the 119 μm line emitted when CH_3OH is pumped by the 9.69 μm P(36) line of the CO_2 laser. The FIR output variations with the mirror vibrating and the chopper turned off are shown in Fig. 21a. These amplitude variations are produced as the pump frequency scans the pump absorption lineshape of the FIR laser. The instantaneous pump frequency, in turn, is determined by the phase condition of the active pump cavity which is periodically varying due to the back injected signal from the vibrating mirror.

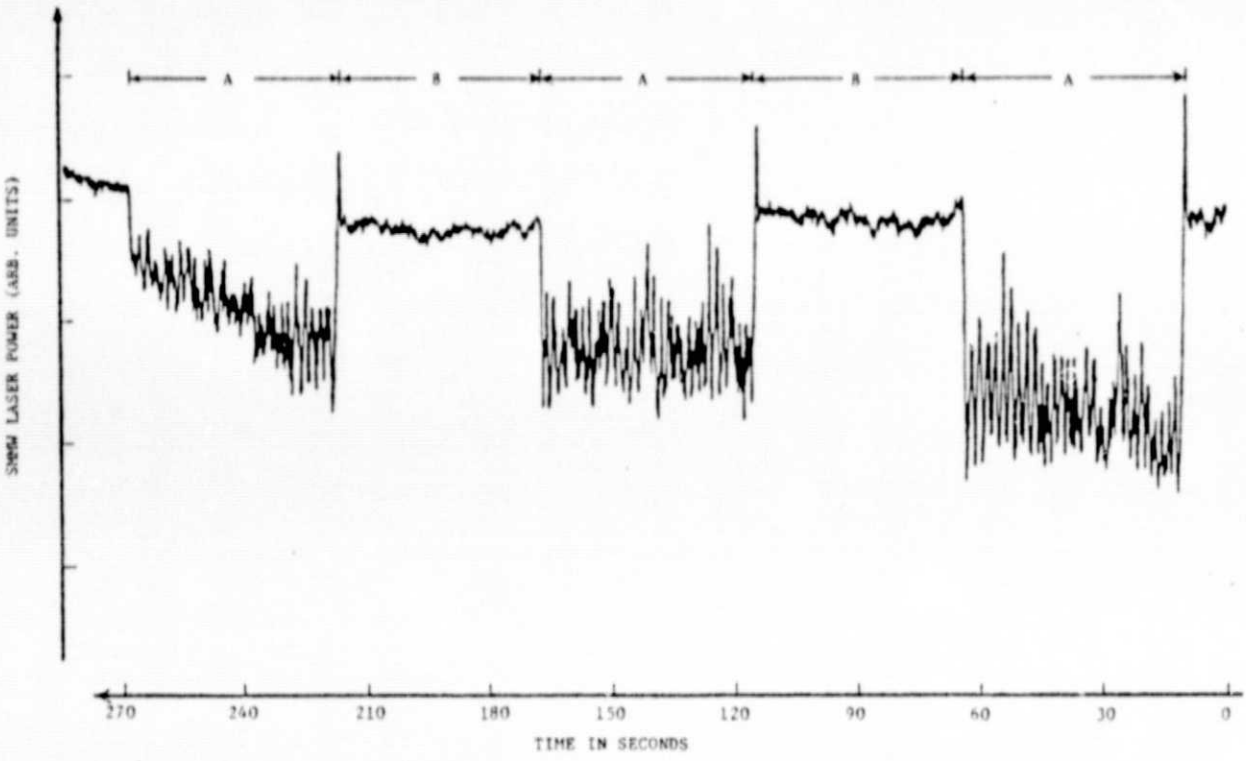

Fig. 20 FIR Output versus time with stationary mirror (A) and with vibrating mirror (B)

With the chopper turned on the FIR output amplitude variations are superimposed on the exponential decay of the pyroelectric response. In Fig. 21b the output exhibits low frequency random amplitude fluctuations with the mirror stationary. In Fig. 21c the amplitude fluctuations have a high frequency component due to the mirror vibration which is approximately 10% of the peak FIR output amplitude and the low frequency random fluctuations are not apparent. It appears that the periodic phase shift in the feedback signal caused by the vibrating mirror serves to reduce the sensitivity of the pump laser to the lower frequency random amplitude and phase fluctuations of the feedback signal. Thus in Fig. 20, using the low frequency response (15 Hz) Golay detector the low frequency fluctuations are significantly reduced when the mirror is vibrating.

a. mirror vibrating
at 100 Hz and
chopper off
Horiz.scale 5 msec/div

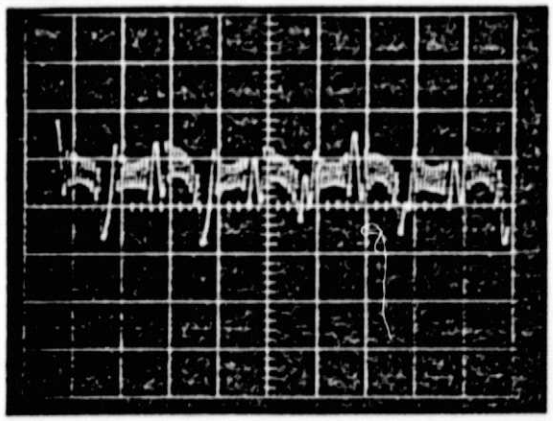

b. mirror stationary
and chopper on
Horiz.scale 20 msec/div

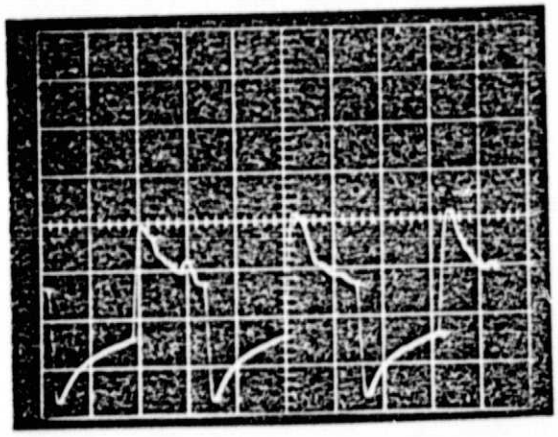

c. mirror vibrating
at 200 Hz and
chopper on
Horiz.scale 20 msec/div

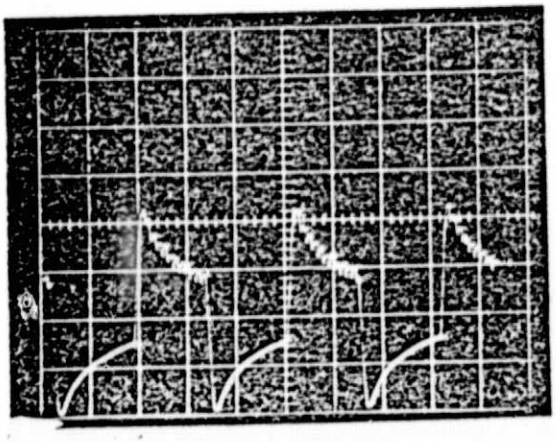

Fig. 21 FIR Output mirror time using pyroelectric detector

With a fast detector, however, the improvement in stability is still significant. The pyroelectric detector is used with the chopper on to obtain the results of Fig. 22. It can be seen that the peaks of each chopper pulse are considerably more uniform in amplitude with the mirror vibrating.

As far as the operation of the pump laser is concerned the phase modulated feedback signal acts as an externally injected signal affecting both the gain and phase conditions for oscillation. The problem of a laser oscillator with an injected signal has received extensive analysis [31-34] usually assuming the injected signal is offset from the unperturbed oscillator frequency. For the present case in which the feedback signal is a phase shifted component at the pump frequency, the pump laser can be modelled as a double Fabry-Perot cavity with one moveable end mirror as shown in Fig. 23.

The pump laser has a single-pass gain $\exp[-i\,k(\nu)\,\ell]$ due to the gain medium located between $x=0$ and $x=\ell$ where ℓ is the fixed mirror separation of the active cavity and $k(\nu) = k'(\nu) - i\,k''(\nu)$ is the frequency dependent complex propagation constant near the lasing transition [35]. The amplitude reflection and transmission coefficients are given by r_i and t_i $(i = 1,2,3)$, respectively. For the configuration of Fig. 23 an assumed initial field amplitude E_i at mirror M2 results in an output field amplitude E_o given by

$$E_o = \frac{r_1 t_2 t_3\, E_i \exp\{-i[2\,k(\nu)\ell + k_o x(t)]\}}{1 - r_1 r_2 \exp[-2i\,k(\nu)\ell] + r_1 r_3 t_2^2 \exp\{-2i[k(\nu)\ell + k_o x(t)]\}} \qquad (8)$$

a. mirror stationary

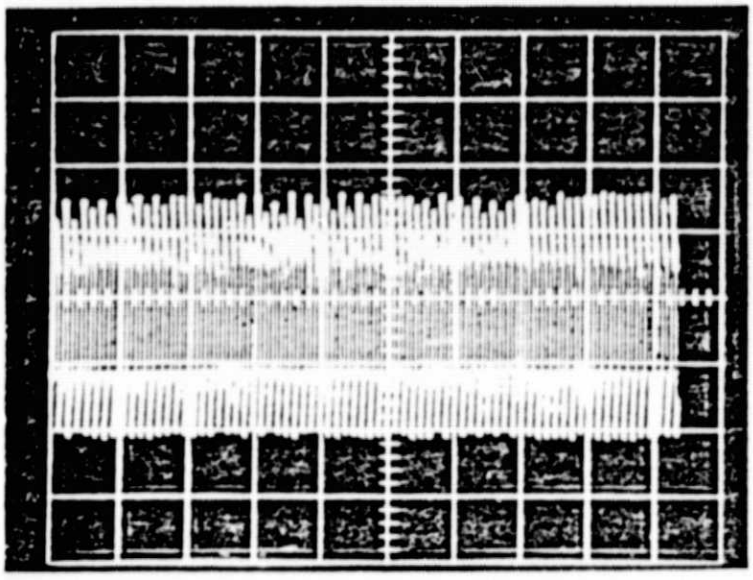

b. mirror vibrating

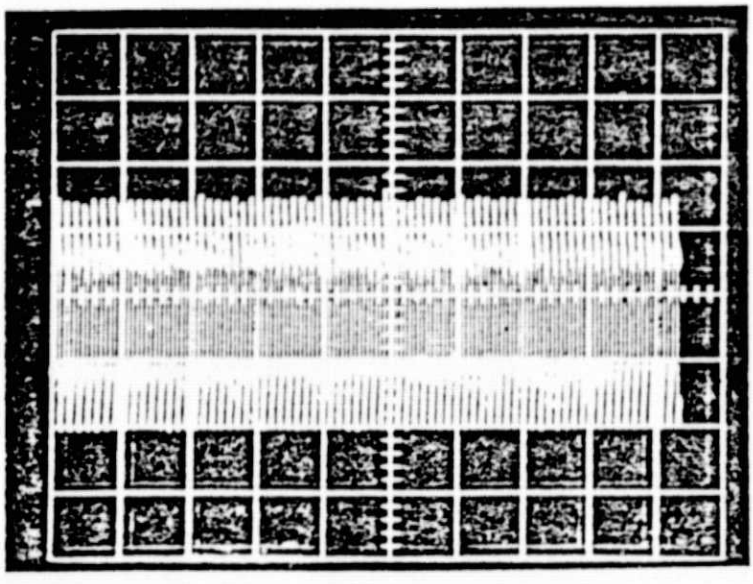

Fig. 22 Amplitude of chopped FIR pulses versus time using pyroelectric detector

where $k_o = 2\pi\nu/c$ is the free space propagation constant. For oscillation to occur for vanishing E_1, the denominator of Eq. (8) is set to zero resulting in amplitude and phase conditions which must be satisfied at threshold. The phase condition is

$$m\pi = k'(\nu)\ell + 0.5 \tan^{-1}\{T \sin 2k_o x(t)/[1 + T \cos 2k_o x(t)]\} \quad (9)$$

where $T = r_3 t_2^2 / r_2$ and m is an integer. Although Eq. (9) was derived at threshold it can be applied more generally using a form for $k'(\nu)$ which includes saturation effects.

Taking $\nu_m = mc/2\ell$ where ν_m is the mth cavity resonance of the laser Eq. (9) can be put in the form

$$\nu_m = \nu[1 + 0.5\,\chi'(\nu)] + cT \sin 2k_o x(t)/\{4\pi\ell[1 + T \cos 2k_o x(t)]\} \quad (10)$$

where $k'(\nu) = k_o[1 + 0.5\,\chi'(\nu)]$ and the approximation $\tan^{-1}\theta \simeq \theta$ has been used since $T \ll 1$. An approximate expression for the peak frequency deviation $\Delta\nu$ can be determined since the extrema of the x-dependent term in Eq. (10) are $\pm cT / (4\pi\ell\sqrt{1-T^2})$.
Taking $\chi'(\nu) = \chi'(\nu_m)$ we find

$$\Delta\nu = (c/2\pi\ell)\ (T/\sqrt{1-T^2})[1 + 0.5\,\chi'(\nu_m)]^{-1} \quad (11)$$

For the experimental configuration of Fig. 4, $\ell = 1.4$ meter and it is estimated that $T = 0.03$. Taking $\chi'(\nu_m) \ll 1$ the peak-frequency deviation is found to be $\Delta\nu \simeq 1$ MHz. This result is consistent with the observations that the pump frequency variations at the order of ±10 MHz are sufficient to quench FIR laser action while the estimated 1 MHz peak frequency deviation of the pump caused by the vibrating mirror produced only a 10% amplitude fluctuation as determined from Fig. 21c.

It has been shown that FIR output amplitude instabilities due to a pump beam back-injected into a pump laser are reduced significantly when a vibrating mirror is used to phase modulate the feedback signal. The peak frequency deviation $\Delta\nu$ of the pump beam due to the phase modulated feedback is given by Eq. (11) and, as expected, is primarily dependent on the amplitude of the pump field coupled back into the pump laser through the factor T.

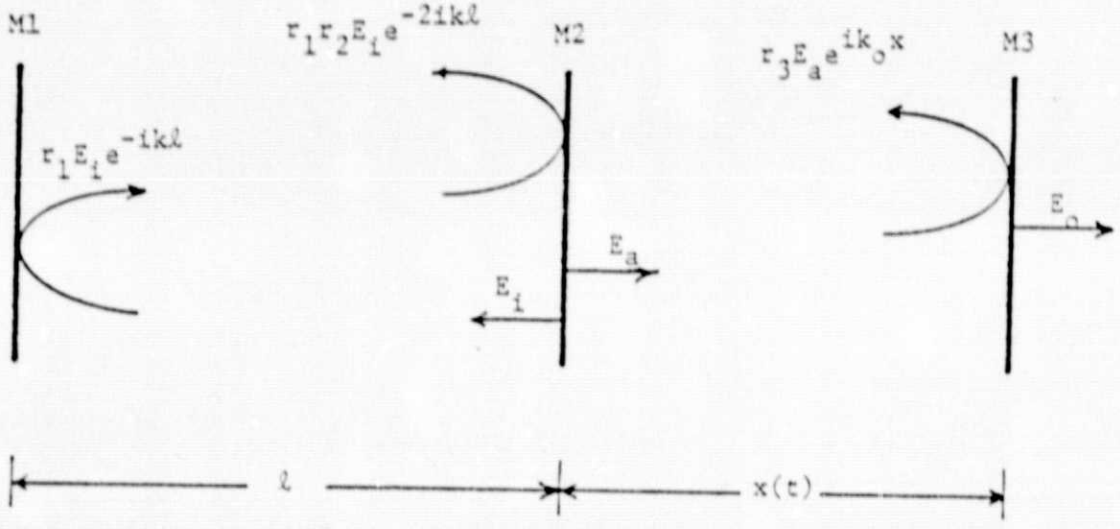

Fig. 23 Double Fabry-Perot cavity used for analysis of phase modulated feedback signal

References

1. D. T. Hodges and T. S. Hartwick, "A Far-Infrared Waveguide Laser," Appl. Phys. Lett., Vol. 23, p. 252, 1973.

2. E. J. Danielewicz, T, K. Plant, and T. A. DeTemple, "Hybrid Output Mirror for Optically Pumped Far Infrared Lasers," Optics Commun., Vol. 13, p. 366, April, 1975.

3. E. J. Danielewicz and P. D. Coleman, "Hybrid Metal Mesh-Dielectric Mirrors For Optically Pumped Far Infrared Lasers," Appl. Opt., Vol. 15, p. 761, March, 1976.

4. M. Schubert, M. Dursechlag and T. A. DeTemple, "Diffraction Limited cw Optically Pumped Lasers," IEEE Jour. Quant. Elec., Vol. QE-13, p. 455, June, 1977.

5. T. Y. Chang and J. D. McGee, "Millimeter and Submillimeter Wave Laser Action in Symmetric Top Molecules Optically Pumped via Parallel Absorption Bands," Appl. Phys. Lett., Vol. 19, p. 103, August, 1971.

6. M. Yamanaka, "Optically Pumped Gas Lasers - a Wavelength Table of Laser Lines," Rev. Laser Engng., Vol. 3, p. 57, 1976.

7. J. J. Gallagher, M. D. Blue, B. Bean, and S. Perkowicz, "Tabulation of Optically Pumped Far Infrared Laser Lines and Applications to Atmospheric Transmission," Infrared Physics 17, p. 43, 1977.

8. M. Rosenbluh, R. J. Temkin and K. J. Button, "Submillimeter Laser Wavelength Tables," Appl. Opt.

9. D. T. Hodges, F. B. Foote, R. D. Reel, "High Power Operation and Scaling Behavior of cw Optically Pumped FIR Waveguide Lasers," IEEE J. Quan. Elec., QE-13, p. 491, June 1977.

10. D. T. Hodges, J. R. Tucker, and T. S. Hartwick, "Basic Physical Mechanisms Determining Performance of the CH_3F Laser," Infrared Physics 16, p. 175, 1976.

11. D. T. Hodges and J. R. Tucker, "Pump Absorption and Saturation in the CH_3F 496 μm Laser," Appl. Phys. Lett 27, p. 667, Dec., 1975.

12. D. T. Hodges, F. B. Foots, and R. D. Reel, "Efficient High-power Operation of the cw Far-infrared Waveguide Laser," Appl. Phys, Lett. 29, p. 662, Nov., 1976.

13. Dean T. Hodges, "cw (Continuous wave) Optically Pumped FIR (Far Infrared) Lasers," Proc. of Soc. of Photo-Optical Inst. Eng., Vol. 105, p. 6, 1977.

14. C. O. Weiss, "Pump Saturation in Molecular Far-Infrared Lasers," IEEE Jour. Quan. Elec., QE-12, p. 580, Oct., 1976.

15. John R. Tucker, "Theory of an FIR Gas Laser," International Conf. on Submillimeter Waves and their applications, Conference Digest, p. 17-18, 1974.

16. J. E. Chamberlain and H. A. Gebbie, "Determination of the Refractive Index of a solid using a Far Infrared Maser," Nature 206, p. 602, 1965.

17. J. J. Lunazzi and M. Garavaglia, "Fabry-Perot Laser interferometry to measure refractive index or thickness of transparent materials," Jour. of Phys. EL Sci. Insts. 5, p. 237, 1973.

18. J. Chamberlain, J. Haigh, and M. J. Hine, "Phase Modulation in Far Infrared (Submillimeter-wave) Interferometers. III - Laser Refractometry," Infrared Physics, Vol. 11, p. 75, 1971.

19. V. N. Smiley, "An Active Interference Filter as an Optical Maser Amplifier," Proc. IEEE, 51, p. 120, Jan., 1963.

20. Charles Freed and Ali Javan, "Standing-Wave Saturation Resonances in the CO_2 10.6 μ Transitions Observed in a low-pressure room-temperature Absorber gas," Appl. Phys. Lett. 17, p. 53, July, 1970.

21. W. H. Thomason and D. C. Elbers, "An Inexpensive Method to Stabilize the Frequency of a CO_2 Laser," (preprint) 1974.

22. E. G. Reid, "Servo Electronics for Optically Pumped FIR Laser," Conf. Digest, Second International Conference and Winter School on Submillimeter Waves and their Applications, p. 160, Dec. 6-11, 1976.

23. G. Busse, E. Basel, and A. Pfaller, "Application of the Opto-Acoustic Effect to the operation of Optically Pumped Far-Infrared Gas Lasers," Appl. Phys. (Springer-Verlag) 12, p. 387, 1977.

24. G. Busse and R. Thurmaier, "Use of the Optoacoustic effect to discover cw far-infrared laser lines," Appl. Phys., Lett 31, p. 194, Aug., 1977.

25. Lars-Goran Rosengran, "Optimal Optoacoustic detector design," Appl. Opt., 14, p. 1960, Aug., 1975.

26. W. Schnell and G. Fischer, "Spectrophone measurements of isotopes of water vapor and nitric oxide and of phosgene at selected wavelengths in the CO and CO_2 laser region," Optics Lett. 2, p. 67, March, 1978.

27. S. P. Belove, A. V. Burenin, L. I. Gershtein, V.V. Korolikhin and A. F. Krupnow, "High Sensitivity Millimeter and Submillimeter wide-range microwave spectroscopy of gases," Opt. Spectroscopy 35, p. 172, Aug., 1973.

28. L. B. Kreuzer, "Ultralow Gas Concentration Infrared Absorption Spectroscopy," Jour. Appl. Phys, 42, p. 2934, June, 1971.

29. T. Y. Chang and C. Lin, "Effects of Buffer gases on an optically pumped CH_3F FIR Laser," J. Opt. Soc. Am. 66, p. 362, April, 1976.

30. T. W. Hansch, K. C. Harvey, G. Meisel, and A. L. Schawlow, "Two-Photon Spectroscopy of Na 3s-4d Without Doppler Broadening Using a cw Dye Laser," Optics Commun. Vol. 11, p. 50, May, 1974.

31. R. H. Pantell, "The Laser Oscillator with an External Signal," Proc. IEEE, Vol. 53, p. 474, May, 1965.

32. C. L. Tang and H. Statz, "Phase-Locking of Laser Oscillations by Injected Signal," J. Appl. Phys., Vol. 38, p. 323, Jan., 1967.

33. C. J. Buczek, R. J. Freiberg and M. L. Skolnick,"Laser Injection Locking," Proc. IEEE, Vol. 61, p. 1411, Oct., 1973.

W. R. Leeb and A. L. Scholtz, "Single Mode Laser Frequency Modulation," IEEE Jour. Quan. Elec., Vol. QE-13, p. 925, Nov., 1977.

35. A. Yariv, "Introduction to Optical Electronics," 2nd. ed., Holt Rinehart and Winston, 1976.